Design of W-band PIN Diode SPDT Switch with Low Loss

Yun Jiang [1], Yuan Ye [1], Daotong Li [2], Zhaoyu Huang [1], Chao Wang [1,*], Jingjian Huang [1], and Naichang Yuan [1]

[1] State Key Laboratory of Complex Electromagnetic Environment Effects on Electronics and Information System College of Electronic Science, National University of Defense Technology, Changsha, 410073, China

[2] Center of Communication and Tracking Telemetry Command, Chongqing University, Chongqing, 400000, China
*sywangc@163.com

Abstract ─ A W-band PIN diode single pole double throw (SPDT) switch with low insertion loss (IL) was successfully developed using a hybrid integration circuit (HIC) of microstrip and coplanar waveguide (CPW) in this paper. In order to achieve low loss of the SPDT switch, the beam-lead PIN diode 3D simulation model was accurately established in Ansys High Frequency Structure Simulator (HFSS) and the W-band H-plane waveguide-microstrip transition was realized based on the principle of the magnetic field coupling. The key of the proposed method is to design the H-plane waveguide-microstrip transition, it not only realizes the low IL of the SPDT switch, but also the direct current (DC) bias of the PIN diode can be better grounded. In order to validate the proposed design method, a W-band PIN diode SPDT switch is fabricated and measured. The measurement results show that the IL of the SPDT switch is less than 2 dB in the frequency range of 85 to 95 GHz, while the isolation of the SPDT switch is greater than 15 dB in the frequency range of 89.5 to 94 GHz. In the frequency range of 92 to 93 GHz, the IL of the SPDT switch is less than 1.65 dB, and its isolation is higher than 22 dB. Switch rise time and switch fall time of the SPDT switch are smaller than 29ns and 19ns, respectively. Good agreement between the simulations and measurements validates the design method.

Index Terms ─ Insertion loss, isolation, PIN diode, SPDT switch, switch fall time, switch rise time, W-band, waveguide-microstrip transition.

I. INTRODUCTION

Driven by wide applications, such as the radio astronomy, radar system, 5G and 6G communication, there has been an increasing interest in developing the SPDT switch working at W-band (75-110 GHz) or high frequency band [1-5]. According to different design processes, the commonly used switches in the W-band include HIC switches [6-8], monolithic microwave integrated circuit (MMIC) switches [9-12], and micro-electromechanical system (MEMS) switches [13-17]. The W-band MMIC switches and MEMS switches technology can realize wide bandwidth and good consistency, but the high loss, low power capacity, difficult processing and complex manufactures are inevitable. The HIC switches were considered as an expedient choice, which is suitable for low ILs, high power capacity, low-cost and mass production. However, the traditional hybrid integrated PIN diode switches are designed based on the principle of the electric field coupling. There are two commonly used methods, one is to use the fin line structure combined with the accurate PIN diode 3D simulation model to design the W-band switch [6], and the other is to use a microstrip line structure [8]. The switch of the fin line structure can achieve good DC bias grounding, but the relatively lager size, high ILs and difficult integrated with other devices are inevitable [7]. At the same time, the switch of the traditional microstrip line structure is easy to integrate with other millimeter wave devices. However, an external DC bias grounding structure is required, which will increase the ILs and size of the switch [8].

With the development of millimeter wave communication, the W-band SPDT switch with high power handling capability, low ILs and low-cost becomes indispensable. In this paper, an accurate PIN diode simulation model is established in Ansys HFSS. A W-band SPDT switch with compact structure, low loss and easy DC bias grounding was designed by using microstrip and CPW structure combined with accurate PIN diode simulation model. The W-band SPDT switch is fabricated, whose simulated and measured results are in good agreement. In the frequency range of 85 to 95 GHz, the IL of the SPDT switch is less than 2 dB, and its isolation is higher than 13 dB.

II. SWITCH STRUCTURE AND DESIGN

Figure 1 shows the schematic diagram of the proposed W-band SPDT switch, which can be seen as composing of two single pole single throw (SPST) circuits. The switches are divided into parallel switch and series switch according to the connection mode of the PIN diode. In this paper, in order to reduce the IL of the SPDT switch, the two PIN diodes are connected in

Submitted On: February 7, 2021
Accepted On: April18, 2021

https://doi.org/10.47037/2021.ACES.J.360712

parallel with the microstrip line at the expense of the switch isolation. As shown in Fig. 1, the D_1 and D_2 are the PIN diode. At the same time, the lengths of L_1 and L_2 equal to quarter wavelength are adopted. As we all know, when the PIN diode is turned on, it exhibits low resistance characteristics, which can be equivalent to a short circuit. The PIN diode is reverse biased, it exhibits high resistance characteristics, which can be equivalent to an open circuit. The impedance characteristics of the PIN diode under different DC biases are used to design the SPDT switch, and then it is matched or mismatched at the millimeter wave input to control the signal on or off [18]. Considering the application of the SPDT switch, the port 1 is adopted the standard wave port WR10, and both of the port 2 and port 3 are matched to 50Ω.

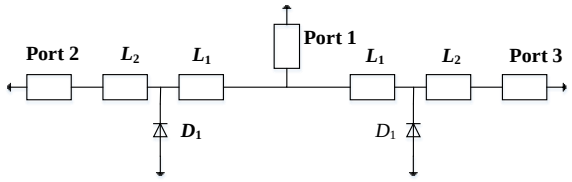

Fig. 1. Schematic of the W-band SPDT switch.

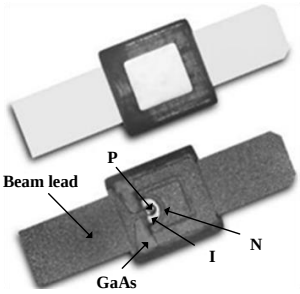

Fig. 2. The physical photo of the PIN diode.

In order to satisfy the needs of different frequencies and designs, the PIN diodes are available in various packaging forms. According to the W-band radar front-end requirements for SPDT switch IL, power capacity, isolation, volume, etc., the selected beam-leaded PIN diode was fabricated by Skyworks using GaAs technology. The physical photo of the PIN diode is shown in Fig. 2. The PIN diode size is 0.31 mm × 0.28 mm × 0.05 mm (length × width × thickness), which is not include the size of the beam lead. The basic parameters of the diode given by the manufacturer are shown in Table 1.

Table 1: The basic parameters of the diode

Reverse Voltage (V)	Max Total Capacitance (10V, 1MHz) (pF)	Max Series Resistance (10mA, 100MHz) (Ω)	Switch Time (I_F=10mA) (ns)
60	**0.025**	**3.5**	**25**

From the SPICE provided by the manufacturer, it is impossible to know the accurate forward and reverse bias impedance parameters of the PIN diode in the W band (85-100 GHz). On the basis of the PIN diode simulation model proposed in [6], the accurate diode model is established in Ansys HFSS. The PIN diode simulation model is shown in Fig. 3. As shown in Fig. 3, the P-region and N-region are equivalent to an ideal electrical conductor. At the same time, the I-region is simulated as the impedance boundary, whose value is 6+j30 in the forward bias state and 130-j570 in the reverse bias state. The package of the PIN diode contains an oxide-nitride passivation layer, copper and GaAs. Finally, the forward and reverse bias impedance parameters of the diode are extracted according to the SPICE provided by the manufacturer and the simulation model of the PIN diode in HFSS.

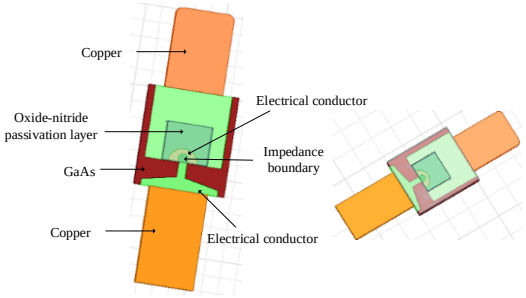

Fig. 3. The simulation model of the PIN diode.

In this section, the W-band H-plane waveguide-microstrip transition will be designed and analyzed based on the principle of the magnetic field coupling. The simulation model and results of the W-band (85-100 GHz) waveguide-microstrip transition are shown in Fig. 4. The metal strips (thickness = 0.017 mm) with different patterns are designed on a Duriod 5880 substrate (thickness = 0.127 mm and ε_r = 2.2) and then inserted into the H-plane of a standard WR10 waveguide cavity. In order to achieve good matching of the H-plane transition structure in the frequency range of 85-100 GHz, two high-impedance lines are added between the probe and the 50 Ω microstrip line. Meanwhile, for good grounding efficiency, the metal strip of the probe at the end must make good contact with the cavity, and the two ground vias must be filled with conductive glue. Finally, the H-plane transition structure can achieve good grounding by the cavity. In the frequency range of 85 to 100 GHz, the simulation results show that the return loss of the H-plane waveguide-microstrip transition is greater than 20 dB, and their IL is less than 0.09 dB. Therefore, the H-plane waveguide-microstrip transition structure not only has a transition effect, but also can achieve a good grounding effect. According to the above

discussion, in the subsequent design of the W-band SPDT switch, the H-plane waveguide-microstrip transition structure can reduce the size and IL of the switch.

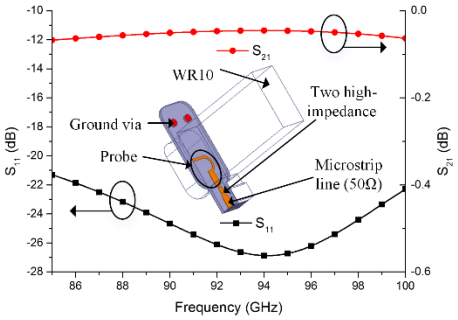

Fig. 4. The simulation model and results of the H-plane waveguide-microstrip transition.

In order to facilitate the measurement of the SPDT switch, an E-plane waveguide-CPW transition is designed. The simulation model and results are shown in Fig. 5. The used substrate is Duriod 5880 substrate with thickness of 0.127 mm and its top includes metal strips having different shapes with thickness of 0.017 mm. The substrate inserted into the central E-plane of a standard WR10 waveguide cavity.

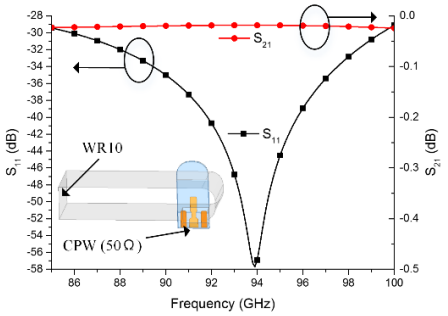

Fig. 5. The simulation model and results of the E-plane waveguide- CPW transition.

In the design of the W-band SPDT switch, in order to avoid the leakage of radio frequency signals due to the addition of a DC bias to the PIN diode, the low pass filter (LPF) in the W-band is designed. The LPF is used to power the diode, and its simulation results and model are shown in Fig. 6. The simulation results show that the LPF has high rejection in the frequency range of 85 to 100 GHz.

In the section, combining all the above designs, the W-band SPDT switch without waveguide-CPW transition is designed, and its simulation results and model are shown in Fig. 7. The substrate size of the SPDT switch without waveguide-CPW transition is 7.47 × 3.44 × 0.16 mm^3.

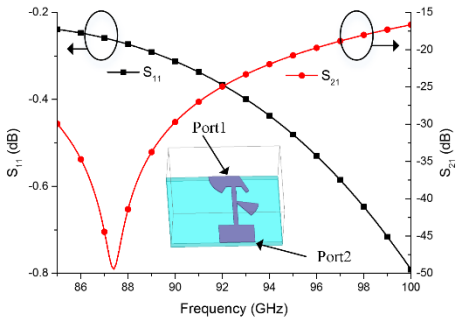

Fig. 6. The simulation model and results of the LPF.

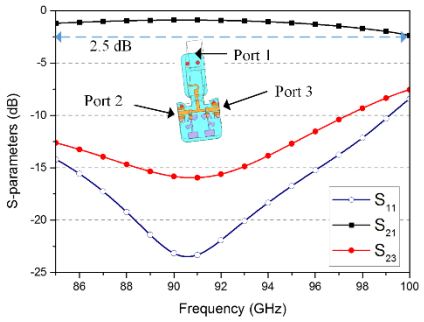

Fig. 7. The simulation model and results of the W-band SPDT switch without waveguide-CPW transition.

In order to facilitate the measurement of W-band SPDT switches, the ports 2 and 3 achieve standard wave port WR10 output through the waveguide-CPW transition. At the same time, a DC power supply board for PIN diodes is designed. The simulation model and results of the W-band SPDT switch with waveguide-CPW transition are shown in Fig. 8. It can be seen from the simulation results that the IL of the SPDT switch is less than 2dB, and its reflection and isolation are greater than 10 dB in the frequency range of 85 to 97 GHz.

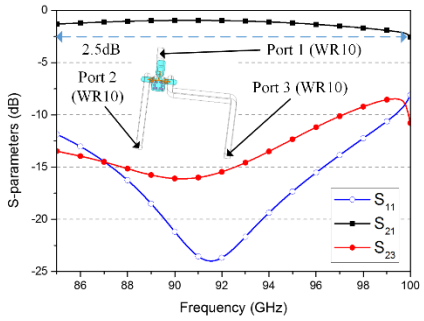

Fig. 8. The simulation model and results of the W-band SPDT switch with waveguide-CPW transition.

III. EXPERIMENTAL RESULTS

According to the analysis and discussion above, a W-band SPDT switch with waveguide-CPW transition is designed, and it is shown in Fig. 9. As shown in Fig. 9 (a), The PIN diode DC bias without the external grounding structure can achieve a good grounding effect only through the H-plane waveguide-microstrip transition. The assembly drawing of the W-band SPDT switch with the waveguide-CPW transition under the microscope is shown in Fig. 9 (b), and its physical photo is shown in Fig. 9 (c).

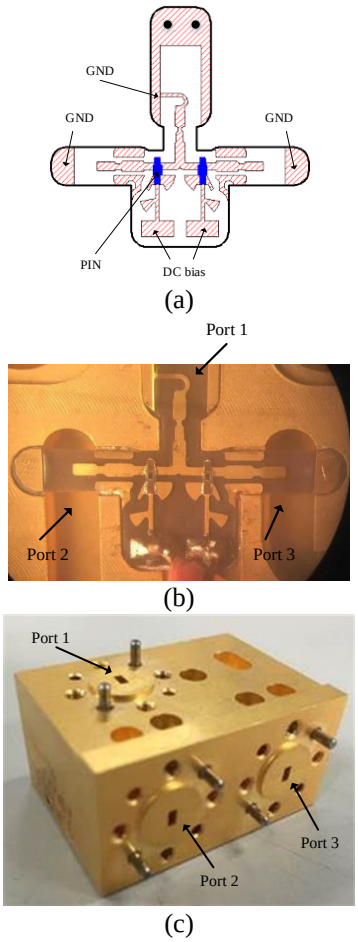

Fig. 9. (a) Fabricated substrate of the SPDT switch, (b) assembly drawing of the SPDT switch, and (c) physical photo of the SPDT switch.

An Agilent 83623B signal source along with Agilent W-band frequency extension modules 8355B and an Agilent 8757D scalar network analyzer were used for S-parameters measurement. In the measurement of the SPDT switch, port 1, port 2, and port 3 correspond to the ports in the simulation model in Fig. 8. The measured results of Fig. 9 (c) are shown in Fig. 10. When port 2 is on and port 3 is isolated, the measurement results of the W-band SPDT switch with waveguide-CPW transition are shown in the Fig. 10 (a). Moreover, when port 3 is on, the measurement results are shown in the Fig. 10 (b). In the frequency range 85 to 95 GHz, the measured ILs of the port 2 is less than 2 dB and its isolation is greater than 12 dB under on-state, as seen in Fig. 10 (a). As shown in Fig. 10 (b), in the frequency range 85 to 96.5 GHz, the measured ILs of the port 3 is less than 2 dB and its isolation is greater than 10 dB under on-state. In the frequency range of 89.5 to 94 GHz, the measured results that the ILs of the SPDT switch are less than 2 dB, while its isolation is greater than 15 dB. In the frequency range of 92 to 93 GHz, the measured ILs of the SPDT switch are less than 1.65 dB, its return losses are greater than 15 dB, and its isolation is greater than 22 dB.

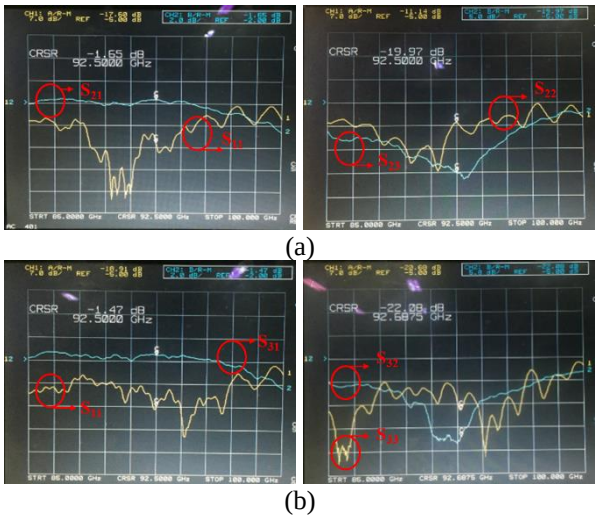

Fig. 10. (a) Measured results of the fabricated SPDT switch port 2, and (b) measured results of the fabricated SPDT switch port 3.

In the test of the SPDT switching time, the radio frequency signal after passing the detector is measured through an oscilloscope. The measured results of the SPDT switching times are shown in Fig. 11. As seen in Fig. 11, switch rise time and switch fall time of the SPDT switch are lower than 29ns and 19ns, respectively.

Table 2 tabulates the performance comparisons of the proposed W-band SPDT switches with some previous works. Compared with the designs in [6] and [14], our proposed one has lower ILs. At the same time, the design in [6] only provides simulation results. Note that the works in [9, 11-12] were used by MMIC technology and tested by GSG probing. Therefore, the ILs of [9, 11-12] in Table 2 were presented without losses of the waveguide-CPW transition. For our design, the IL in Table 2 has included the loss of the waveguide-CPW transition back to back, which is about 0.7 dB at the frequency range of 89.5-94 GHz.

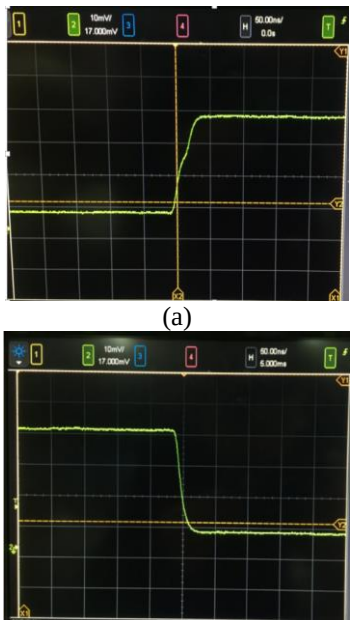

(a) (b)

Fig. 11. (a) Measured results of the SPDT switch rise time, and (b) measured results of the SPDT switch fall time.

Table 2: Performance comparisons with some previous W-band SPDT switches

	Technology	Frequency (GHz)	IL (dB)	Isolation (dB)	Ports
[6]	HIC	85-95	1.3-2.5	17.5-24	WR10
[9]	MMIC	75-110	1.4-2	19-22	CPW
[11]	MMIC	75-110	1.2-1.6	17.7-20	CPW
[12]	MMIC	75-110	1-1.6	28.5-31.6	CPW
[14]	MEMS	75-80	9.1-11	22-25	CPW
This work	**HIC**	**89.5-94**	**1.47-2**	**15-22**	**WR10**

IV. CONCLUSION

Based on the principle of the magnetic field coupling, a W-band PIN diode SPDT switch with low IL has been presented using the HIC of microstrip and CPW in this paper. By designing H-plane waveguide-microstrip transition and the accurate models of PIN diode, low ILs and compact structure can be achieved. Finally, the simulations and measurements of the demonstrative W-band SPDT switch are in good agreement. The measured ILs of the SPDT switch are less than 1.65 dB, its return losses are greater than 15 dB, and its isolation is greater than 22 dB, in the frequency range of 92 to 93 GHz.

REFERENCES

[1] A. Morales, O. Gallardo, J. J. V. Olmos, and I. T. Monroy, "Beam steering application for W-band data links with moving targets in 5G wireless networks," *Journal of Communications and Information Networks*, vol. 2, no. 2, pp. 91-100, June 2017.

[2] Y. J. Guo, K. D. Xu, X. J. Deng, X. Cheng, and Q. Chen, "Millimeter-wave on-chip bandpass filter based on spoof surface plasmon polaritons," *IEEE Electron Device Letters*, vol. 41, no. 8, pp. 1165-1168, Aug. 2020.

[3] K. D. Xu, X. Zhu, Y. Yang, and Q. Chen, "A broadband on-chip bandpass filter using shut dual-layer meander-line resonators," *IEEE Electron Device Letters*, vol. 41, no. 11, pp. 1617-1620, Oct. 2020.

[4] D. Li and K. Xu, "Multifunctional switchable filter using coupled-line structure," *IEEE Microw. Wireless Compon. Lett.*, Early Access, 2021. DOI: 10.1109/LMWC.2021.3067893.

[5] I. F. Akyildiz, A. Kak, and S. Nie, "6G and beyond: The future of wireless communications systems," *IEEE Access*, vol. 8, pp. 133995-134030, June 2020.

[6] S. H. Jia and W. Xue, "Design of W-band SPDT switch by employing full-wave EM simulator," *2012 IEEE International Conference on Computational Problem-Solving (ICCP)*, Leshan, China, pp. 425-427, Oct. 2012.

[7] S. H. Jia and Y. H. Zhang, "W-band finline SPST switch," *2012 IEEE International Conference on Computational Problem-Solving (ICCP)*, Leshan, China, pp. 248-250, Oct. 2012.

[8] Z. B. Xu, J. Guo, C. Qian, and W. B. Dou, "Analysis and design of a novel W-band SPST switch by employing full-wave EM simulator," *Journal of Infrared. Millimeter. and Terahertz Waves*, vol. 32, no. 12, pp. 1434-1445, Dec. 2011.

[9] P. Song, R. L. Schmid, A. C. Ulusoy, and J. D. Cressler, "A high-power, low-loss W-band SPDT switch using SiGe PIN diodes," *2014 IEEE Radio Frequency Integrated Circuits Symposium*, Tampa, FL, USA, pp. 195-198, June 2014.

[10] X. J. Bi, M. Annamalai, Arasu, Y. Zhu, and M. Je, "A low switching-loss W-band radiometer utilizing a single-pole-double-throw distributed amplifier in 0.13-μm SiGe BiCMOS," *IEEE Trans. Microw. Theory Tech.*, vol. 64, no. 1, pp. 226-238, Jan. 2016.

[11] F. Thome, E. Ture, P. Brückner, R. Quay, and O. Ambacher, "W-band SPDT switches in planar and tri-gate 100-nm gate-length GaN-HEMT technology," *2018 German Microwave Conference (GeMIC)*, Freiburg, Germany, pp. 331-334, Mar. 2018.

[12] F. Thome, A. Leuther, and O. Ambacher, "Low-loss millimeter-wave SPDT switch MMICs in a metamorphic HEMT technology," *IEEE Microw. Wireless Compon. Lett.*, vol. 30, no. 2, pp. 197-200, Feb. 2020.

[13] J. Rizk, G. L. Tan, J. B. , and G. M. Rebeiz, "High-

isolation W-band MEMS switches," *IEEE Microw. Wireless Compon. Lett.*, vol. 11, no. 1, Jan. 2001.
[14] S. M. Sim, Y. Lee, Y. H. Jang, Y. S. Lee, Y. K. Kim, I. L. Garro, and J. M. Kim, "A 50-110 GHz ohmic contact RF MEMS silicon switch with dual axis movement," *Microelectronic Engineering*, vol. 162, pp. 69-74, May 2016.
[15] A. Kapoor, P. K. Shrivastava, S. K. Koul, and A. Basu, "Back to back wide-band CPW-to-waveguide transition with RF MEMS shunt switch in W-band," *2019 IEEE International Conference on Microwaves. Antennas. Communications and Electronic Systems (COMCOS)*, Tel-Aviv, Israel, pp. 1-6, Nov. 2019.
[16] M. H. Koh and A. E. Grant, "High power amplifier design with RF-MEMS output switch using SonnetTM," *2012 International Applied Computational Electromagnetics Society Symposium (ACES)*, Columbus, Ohio, USA, pp. 10-14, Apr. 2012.
[17] S. Suganthi, K. Murugesan, and S. Raghavan, "CPW dependent loss analysis of capacitive shunt RF MEMS switch," *Applied Computational Electromagnetics Society Journal*, vol. 31, no. 4, pp. 410-416, Apr. 2016.
[18] A. Tang, T. Reck, R. Shu, L. Samoska, Y. Ye, Q. Gu, B. J. Drouin, J. Truettel, R. A. Hadi, Y. Xu, S. Sarkozy, R. Lai, M. C. F. Chang, and I. Mehdi, "A W-band 65nm CMOS/InP-hybrid radiometer & passive imager," *2016 IEEE MTT-S International Micro-wave Symposium (IMS)*, San, Francisco, CA, USA, pp. 1-3, May 2016.

Yun Jiang was born in Hunnan Provence, China. He received the M.S. degrees in Electronic Engineering from the University of Electronic Science and Technology of China (UESTC), Chengdu, China, in 2017, and currently he is working toward the Ph.D. degree in National of Defense University. His research interests include RF/millimeter-wave components and circuits.

Yuan Ye was born in Guangxi, China. She received the M.S. degree in Sun Yat-sen University, Guangzhou, China, in 2012, and currently she is working toward the Ph.D. degree in National University of Defense Technology. Her current research interests include ultra-wideband antenna Arrays and reconfigurable antenna.

Daotong Li (S'15-M'16) received the Ph.D. degree in Electromagnetic Field and Microwave Technology from the University of Electronic Science and Technology of China (UESTC), Chengdu, China, in 2016.

He is currently an Associate Professor with the Center of Communication and Tracking Telemetry Command, Chongqing University, Chongqing. Since 2015, he has been a Visiting Researcher with the Department of Electrical and Computer Engineering, University of Illinois at Urbana–Champaign, Urbana, IL, USA, with financial support from the China Scholarship Council. He has authored or coauthored over 70 peer-reviewed journal or conference papers.

His current research interests include RF, microwave and millimeter-wave technology and applications, microwave power transmission (MPT), antennas, devices, circuits and systems, and passive and active (sub-) millimeter-wave imaging and radiometer. Li was a recipient of the UESTC Outstanding Graduate Awards by the Sichuan province and UESTC in 2016. He was a recipient of the National Graduate Student Scholarship from the Ministry of Education, China, and "Tang Lixin" Scholarship. He is serving as a Reviewer for several IEEE and IET journals, and many international conferences as a TPC Member, a Session Organizer, and the Session Chair.

Zhanyu Huang was born in 1992. He received the M.S. degree in Electronics and Communication Engineering from the University of Electronic Science and Technology of China, Chengdu, China in 2018, where he is currently pursuing Ph.D. degree with the College of Electronic Science and Engineering, National University of Defense Technology, Changsha, China. His current research interests include passive RF/microwave circuits, microstrip antennas and wireless communication.

Chao Wang was born in 1977. He received the Ph.D. degree from the National University of Defense Technology, Changsha, in 2007. He is currently an Associate Professor with the National University of Defense Technology. His research interest is electronic system design.

Jinjian Huang is now working in National University of Defense Technology. He received the Ph.D. degree of Electronics Science and Technology from National University of Defense Technology, Changsha, China in 2014. His research interests include ultra-wide band antenna and phase array antenna.

Naichang Yuan was born in Anhui, China, in 1965. He received the M.S. and Ph.D. degrees in Electronic Science and Technology from the University of Electronic Science and Technology of China in 1991 and 1994, respectively. He is currently a Professor with the National University of Defense Technology. His research interests include array signal processing, radar system design, SAR/ISAR imaging and electronic countermeasures.